Supplementary Information for

γ-Glutamyltranspeptidase and pH based "AND" logic gate fluorescence probe for orthotopic breast tumor imaging

Li-Na Zhang,[a] Hong Zhang,[a] Shan-Yong Chen*[a] Yan-Zhao Liu,[a] Xiao-Hua Yang,[a] Fei-Fan Xiang,[a] Yan-Hong Liu,[a] Kun Li*[a] and Xiao-Qi Yu[a, b]

[a] Key Laboratory of Green Chemistry and Technology, Ministry of Education, College of Chemistry, Sichuan University, Chengdu, 610064, China.

[b] Asymmetric Synthesis and Chiral Technology Key Laboratory of Sichuan Province, Department of Chemistry, Xihua University, Chengdu 610039, China.

E-mail: chensy@scu.edu.cn; kli@scu.edu.cn

Contents

1. Synthesis of Si-NH_2-Glu

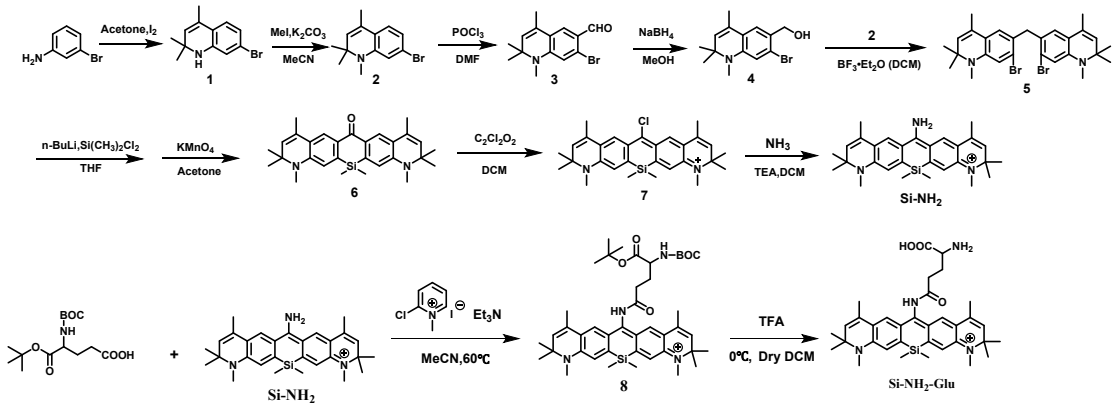

Scheme S1. Synthesis of **Si-NH_2-Glu**

Intermediates **1 to 5** were synthesized according to literature procedures.[1]

Synthesis of 6

To a 50 mL well-dried two necked bottle flushed with argon, compound **5** (970 mg, 1.79 mmol) and dry THF (20 mL) were added. The solution was cooled to -78 °C, n-BuLi (2. 5 M in n-hexane, 1.50 mL, 3.94 mmol) was added and the reaction mixture was stirred a t -78 °C for 2h. Dichlorodimethylsilane (0.24 mL, 1.97 mmol) was added dropwise at –78 °C for 30 min and the reaction mixture was slowly warmed to room temperature. After st irred overnight, the mixture was extracted with DCM and concentrated under vacuum. The solid was dissolved in acetone, stirred at -5 °C for 10 min, then Potassium permanganate (848 mg, 5.37 mmol) was slowly added to the solution. After stirred at room temperature for 4h, the solution was treated with Celite to remove Manganese dioxide then concentrate d under vacuum. The residue was purified by column chromatography on silica gel (DCM: MeOH) to afford compound **6 (**245 mg, 30%). ^{1}H NMR (400 MHz, $CDCl_3$) δ 8.18 (s, 2H), 6.56 (s, 2H), 5.32 (s, 2H), 2.94 (s, 6H), 2.07 (s, 6H), 1.37 (s, 12H), 0.45 (s, 6H). ^{13}C N MR (100 MHz, $CDCl_3$) δ 185.3, 146.9, 140.8, 129.9, 129.8, 128.2, 124.9, 123.4, 112.5, 5 7.3, 31.2, 28.8, 18.9, -0.9.

Synthesis of 7

The compound **6** (183 mg, 0.4 mmol) was dissolved in dry DCM and the Oxalyl chloride (0.34 mL， 4.0 mmol) was dripped into the solution, then stirred at 45 °C for 1h. After concentrated under vacuum, the crude product was used in the next step without further p urification.

Synthesis of 8

To a 50 mL well-dried flask, Boc-L-glutamic acid 1-tert-butyl ester (30 mg, 0.09853 mmol), Triethylamine (0.15 mL), 2-Chloro-1-methylpyridinium iodide (25.17 mg, 0.09853 mmol) and acetonitrile (20 mL) were added then stirred at room temperature for 30 min. The Si-NH_2 was added to the mixture and stirred at 60 °C overnight. The residue, concentrated under vacuum, was purified by column chromatography on silica gel (DCM: MeOH) to afford compound **8** (66.7 mg, 76%). ^{1}H NMR (400 MHz, $CDCl_3$) δ 7.65 (s, 2H), 6.57 (s, 2H), 5.29 (s, 2H), 5.09 (d, J = 8.2 Hz, 1H), 4.09 – 4.01 (m, 1H), 2.89 (s, 6H), 2.34 (ddd, J = 21.0, 10.8, 5.4 Hz, 2H), 1.97 (s, 6H), 1.37 (s, 9H), 1.34 (s, 12H), 1.33 (s, 9H), 0.44 (s, 6H). ^{13}C NMR (100 MHz, $CDCl_3$)) δ 173.9, 171.3, 156.8, 152.0,

150.8, 132.2, 129.6, 127.3, 126.5, 124.4, 120.8, 61.7, 53.1, 33.3, 32.5, 29.1, 27.0, 18.4, -1.3.

Synthesis of compound Si-NH_2

Compound 7 (0.4 mmol) and Triethylamine (1 mL) were dissolved in dry DCM, and NH_3 (in dioxane, 0.4M, 11 mL) was added. The product, concentrated under vacuum, was pure enough to be used directly in the next step. ^{1}H NMR (400 MHz, $CDCl_3$) δ 8.00 (s, 2H), 6.58 (s, 2H), 5.32 (s, 2H), 2.95 (s, 6H), 2.17 (s, 6H), 1.39 (s, 12H), 0.41 (s, 6H). ^{13}C NMR (100 MHz, $CDCl_3$) δ 168.2, 148.3, 142.5, 130.1, 127.9, 124.1, 123.8, 121.4, 113.8, 58.1, 31.4, 29.2, 19.4, -1.4. ESI (+)-HRMS (m/z): $[M]^+$calcd. for: 456.2830, found: 456.2829

Synthesis of compound Si-NH_2-Glu

Compound 8 (20 mg) was dissolved in dry DCM (1.5 mL), then trifluoroacetic acid (0.1 mL) was dripped into the solution and stirred at 0 °C overnight. The mixture was concentrated under vacuum to get the pure product **Si- NH_2-Glu**. ^{1}H NMR (400 MHz, CD_3OD) ^{1}H NMR (400 MHz, CD_3OD) δ 7.55 (s, 2H), 7.14 (s, 2H), 5.63 (s, 2H), 4.12 (t, J = 6.7 Hz, 1H), 3.29 (s, 6H), 2.99 (t, J = 7.3 Hz, 2H), 2.34 (q, J = 7.1 Hz, 2H), 2.03 (s, 6H), 1.52 (s, 12H), 0.55 (s, 6H). ^{13}C NMR (100 MHz, CD_3OD) δ 174.5, 171.3, 156.8, 152.0, 150.8, 132.2, 129.6, 127.3, 126.5, 124.4, 120.8, 61.7, 53.6, 33.3, 32.5, 29.1, 27.0, 18.4, -1.3. ESI (+)-HRMS (m/z): $[M]^+$calcd. for: 585.3255, found: 585.3260

2. Mechanism investigation

A

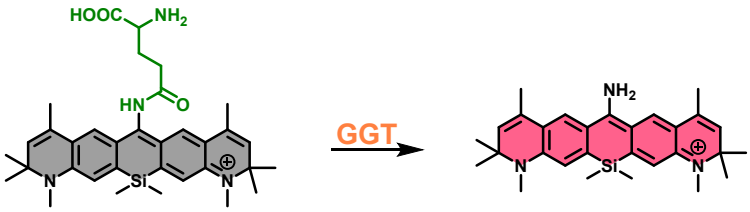

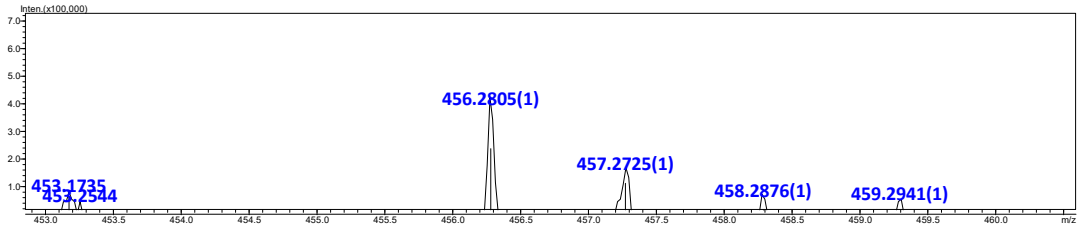

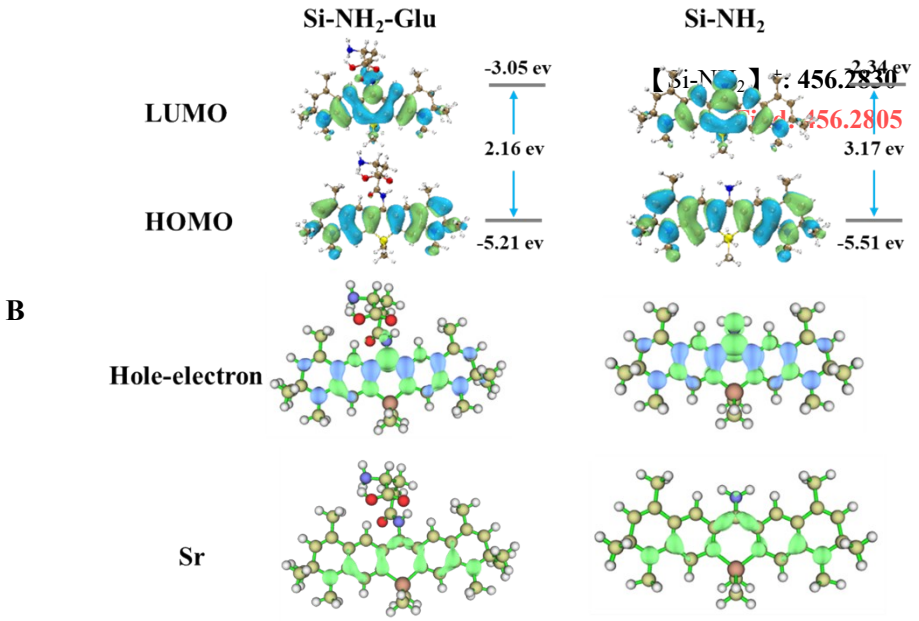

B

ESI+ C

	D index	Sr	EDI
Si-NH_2-Glu	0.225 Angstrom	0.678 a.u.	7.48
Si-NH_2	0.578 Angstrom	0.616 a.u.	8.40

D index: The distance between the hole and the electron's center of mass

Sr: The function of the overlap between electron and hole distributions. The larger the index is, the higher the overlap degree of hole and electron is. The smaller the value, the more significant the hole and electron separation.

EDI (electron delocalization index): The smaller the value, the higher the degree of electron delocalization, that is, the more uniform the distribution[2, 3]

$$D\ index = \sqrt{(X_{ele} - X_{hole})^2 + (Y_{ele} - Y_{hole})^2 + (Z_{ele} - Z_{hole})^2}$$

$$Sr\ index = \sqrt{\rho^{hole}(r)\rho^{ele}(r)dr}$$

$$EDI = 100 \times \sqrt{\int [\rho^{ele}(r)]^2 dr}$$

Figure S1. (A) Mass spectra of **Si-NH_2-Glu** with GGT, (B) The HOMO/LUOM orbits, the hole-electron overlap and Sr function acquired by optimizing ground-state and excited-state geometries at the B3LYP/6-31G** and CAM-B3LYP/6-31G(d) TD levels, respectively. (C) the summarizing of relevant parameter.

3. Spectrum

Figure S2. (A) Normalized absorption spectra of **Si-NH$_2$-Glu** (10 μM) and **Si-NH$_2$-Glu** (10 μM) reacting with GGT (1.5 U/mL) in PBS (pH 7.4). (B) Absorbance spectra of **Si-NH$_2$-Glu** (10 μM) after incubating with GGT (0 - 2 U/mL) for 2h. (C/D) Absorbance (744 nm/515 nm) values dependent on GGT concentration. All experiments were conducted in PBS, pH 7.4, at 37 °C.

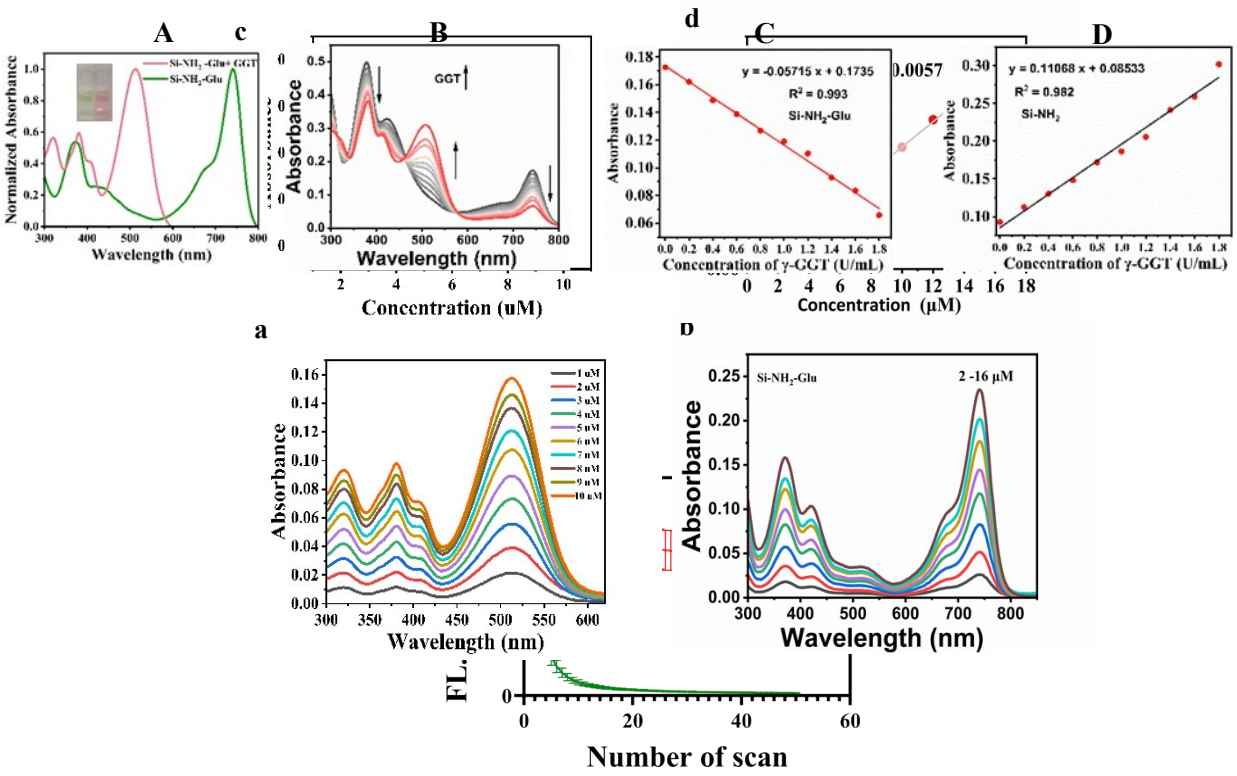

Figure S3. (a/b) UV spectra of **Si-NH$_2$ / Si-NH$_2$-Glu** at different concentrations in PBS. (c/d) Absorption-concentration curve of **Si-NH$_2$ / Si-NH$_2$-Glu** in PBS**.**

Figure S4. Fluorescence intensities of **Si-NH$_2$** (2 μM) and Lysotracker Green (2 μM) in 4T-1 cells continuously irradiated by 100% laser of 543 nm and 488 nm respectively. Green channel: λ_{ex} = 488 nm, λ_{em} = 521 nm. Red channel: λ_{ex} = 543 nm, λ_{em} = 654 nm

	λab (nm)	λem (nm)	ε (M-1cm-1)	Φ (%)				
				MeOH	DMSO	PBS pH 7.4	PBS pH 3.0	PBS pH 9.0
Si-NH2-Glu	744	774	1.5×104	4.8	10.66	2.17	2.35	< 0.01
Si-NH2	515	654	2.6×104	52.53	72.7	23.4	12.4	5.4

Table 1. Photophysical properties of **Si-NH$_2$-Glu** and **Si-NH$_2$**.

4. Limit of detection (LOD)

Limit of Detection (LOD) = 3 × S.D./m

= 3 × 0.10176/5.93901

= 0.0514 U/mL

S.D.: the standard deviation of blank measurements, n = 13,

m: the slope of the linear equation

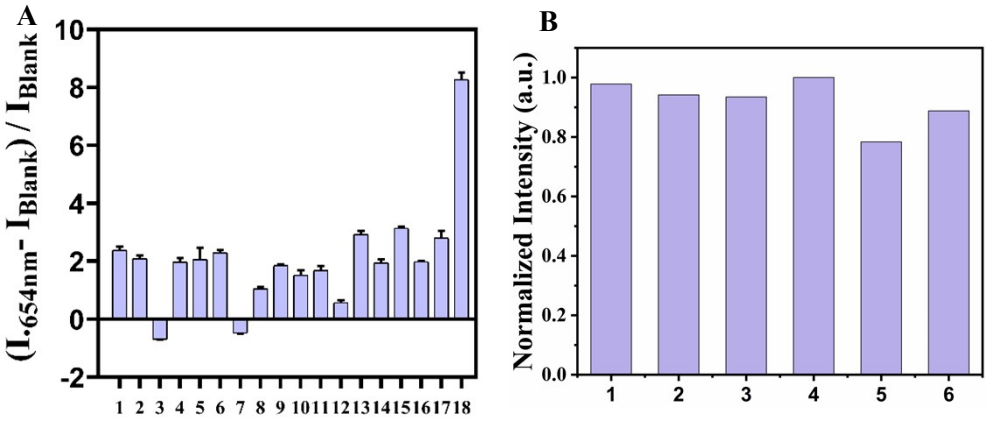

5. Selectivity of Si-NH_2-Glu

Figure S5. (A) Fluorescence response of **Si-NH_2-Glu** (10 μM in PBS) to various analytes, and the solution was incubated for 4 h. 1: blank, 2-6: Ca^{2+}, Cu^{2+}, Fe^{2+}, Mg^{2+}, Zn^{2+} (100 μM), 7-11: $^1O_2$, ClO^-, H_2O_2, ·OH, $ONOO^-$ (100 μM), 12: GSH (1.0 mM), 13: Hcy (100 μM), 14-17: β-Gal, MAO-A, NQO1, NTR (1 μg/mL), 18: γ-GGT (0.1 U/mL). (B) Normalized fluorescence intensity (at 654 nm) of 10 μM **Si-NH_2-Glu** in phosphate buffer solution (50 mM, pH 7.4) to diverse other enzymes. 1, GGT (0.5 U/mL); 2. GGT + MAO-A (0.5 U/mL, 1 μg/mL); 3. GGT + NTR (0.5 U/mL, 1 μg/mL); 4. GGT + CTSB (0.5 U/mL, 1 μg/mL); 5. GGT + AChE (0.5 U/mL, 50 U/mL). $\lambda_{ex/em}$ = 515/654 nm.

6. Cell viability

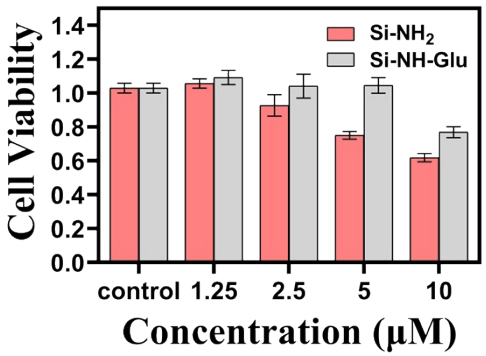

Figure S6. Cellular toxicity assay for **Si-NH_2-Glu** and **Si-NH_2** (1.25-10 μM, 24 h), conducted using CCK-8 (Cell Counting Kit-8) toward 4T-1 cell line.

7. GGT inhibition experiment

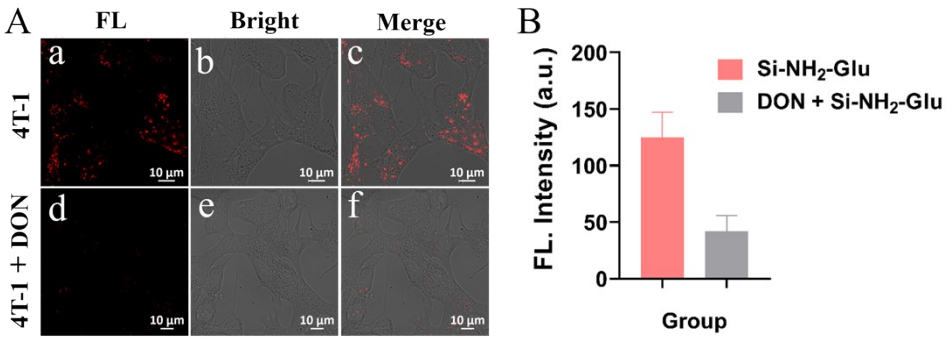

Figure S7. (A) 4T-1 cells treated with **Si-NH_2-Glu** (2 μM) for 30 min (a-c). 4T-1 cells pre-treated with a GGT inhibitor (DON, 1 mM) for 60 min (d-f), and then loaded with **Si-NH_2-Glu** (2 μM) for 30 min at 37 °C. (B) Fluorescence intensity of (a) and (d). Scale bars, 10 μm. λ_{ex} = 543 nm, λ_{em} = 600−700 nm.

8. Co-localization experiment

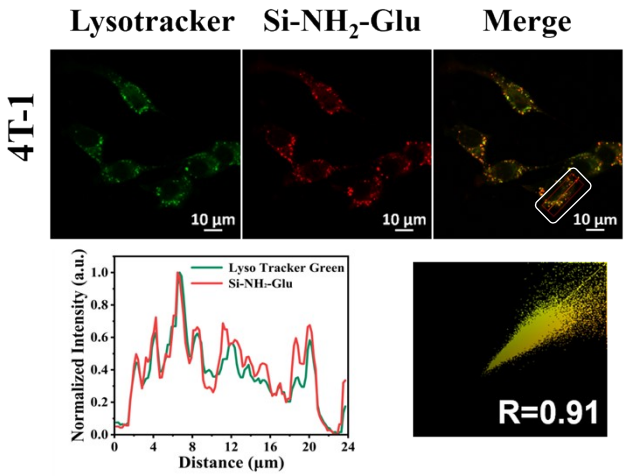

Figure S8. Confocal laser scanning microscopic images of 4T-1 cells treated with 2 μM **Si-NH_2-Glu** and 1 μM Lysotracker Green for 30 min, at 37 °C. Green channel: λ_{ex} = 488 nm, λ_{em} = 490-530 nm. Red channel: λ_{ex} = 543 nm, λ_{em} = 600-700 nm. Scale bar: 10 μm.

9. 3D 4T-1 cell imaging

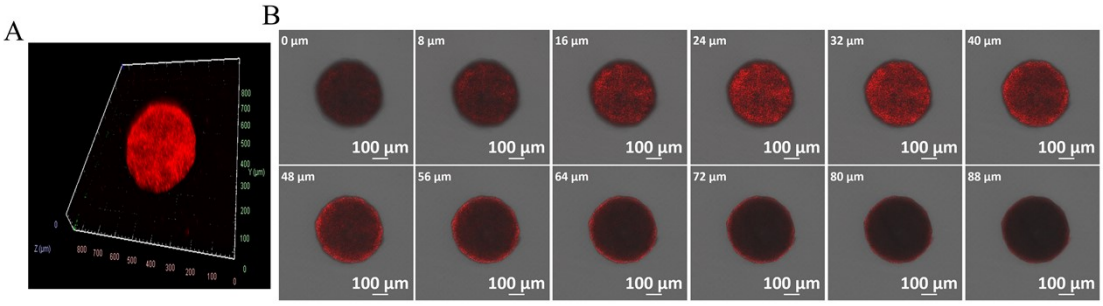

Figure S9. (A) Z-scan images of whole 3D tumor spheroids incubated with **Si-NH$_2$-Glu** (5 μM) for 12 h at 37°C. (B) Z-scan images of every 4 μm section from top to bottom. The image in figure (A) and (B) was taken using a 10× objective lens. λ_{ex} = 543 nm, λ_{em} = 600−700 nm. Scale bar=100 μm.

10. Establishment Mouse Tumor Model

15-20g Balb/c mice aged 4-6 weeks were purchased from Chengdu Senwell Experimental Company (Chengdu, China). 100 μL of 4T-1 cell suspension (1×10^6 cells) were subcutaneous injected into each mouse to establish the tumor models. [4] The animal experiments were carried out according to the protocol approved by the Ministry of Health in the People's Republic of PR China and were approved by Ethical Committees of West China School of Stomatology, Sichuan University (KS2022234).

11. Fluorescence imaging of orthotopic breast tumor mouse models

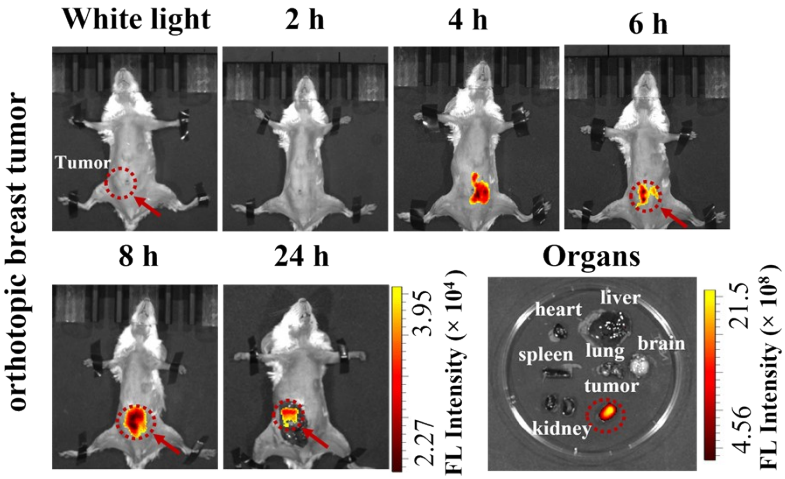

Figure S10. Fluorescence imaging of orthotopic breast tumor mouse models. Representative white light and fluorescence images of the mouse after being given an intravenous injection of 100 μM **Si-NH$_2$-Glu** in 100 μL saline solution. The separated organs and tumor from sacrificed orthotopic tumor mouse model.

12. Hematoxylin-eosin (HE) staining for organs and tumor

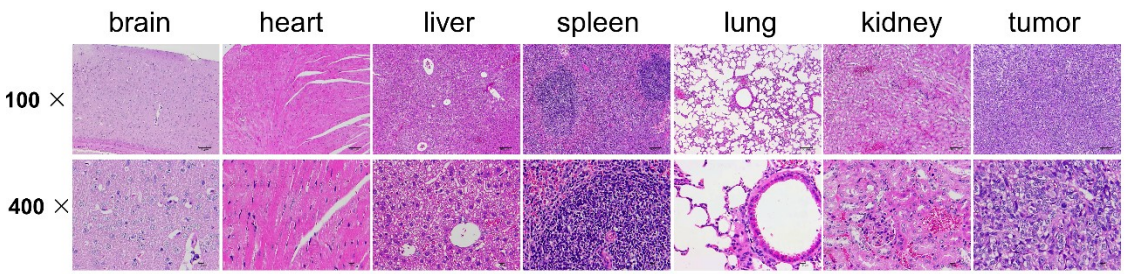

Figure S11. In the organ tissue sections of mice, the nuclei are clearly visible; the cytoplasm and nuclei are in sharp contrast; and there is no obvious change in the tissue morphology, which proves that the probe has good biocompatibility. A small amount of tumor cell necrosis was seen in the tumor tissue; and the necrotic area accounted for less than 5% of the total tumor tissue area. In the tumor growth area, the tumor cells are arranged irregularly; the cytoplasm of the tumor cells is abundant; the nucleus has atypia; and pathological mitoses can be seen.

13. NMR Data

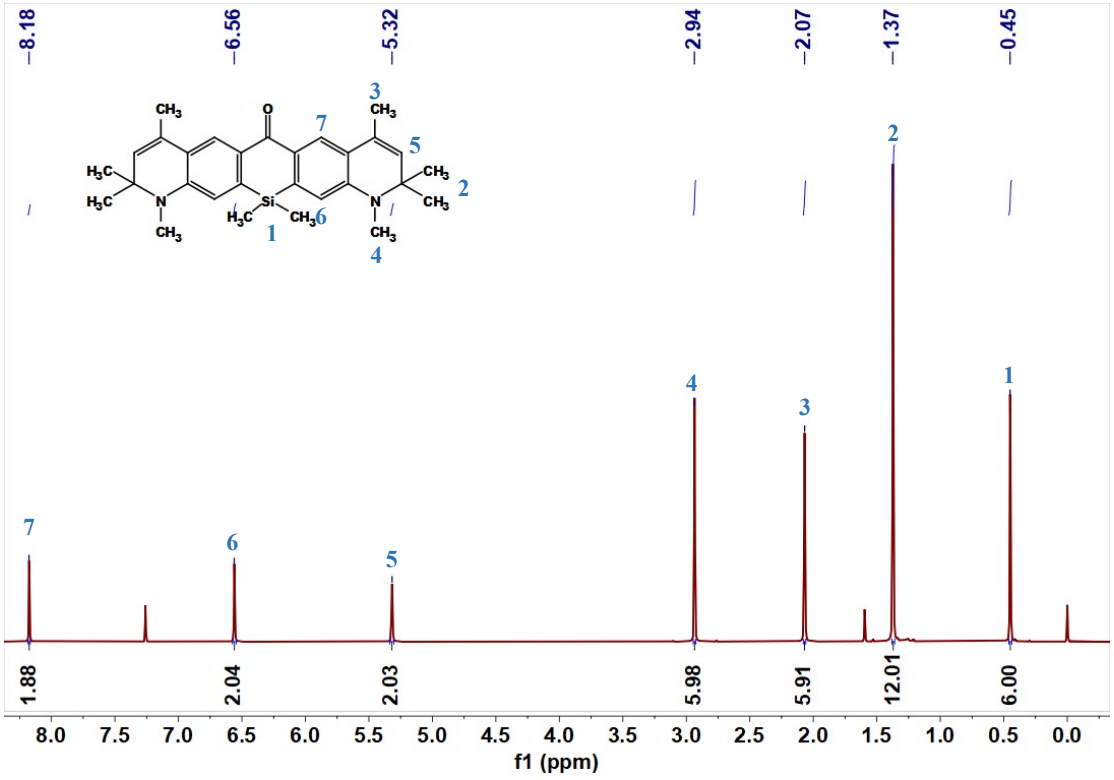

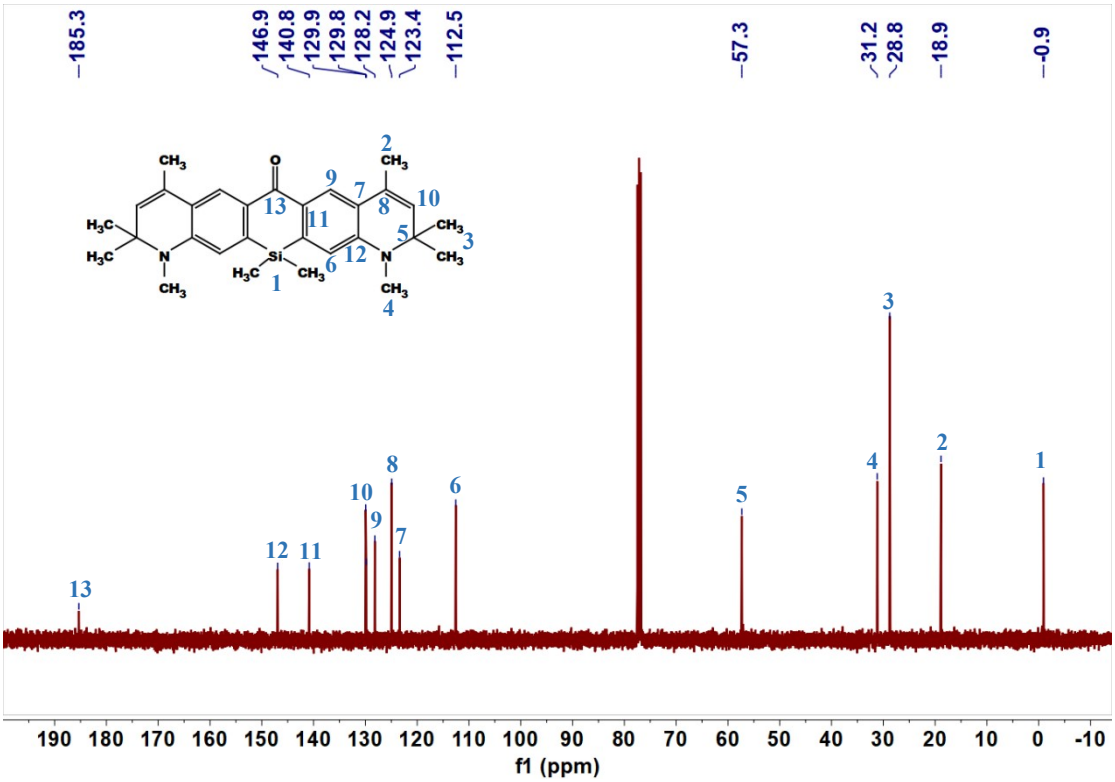

^{1}H NMR of Compound **6** in $CDCl_3$

^{13}C NMR of Compound **6** in $CDCl_3$

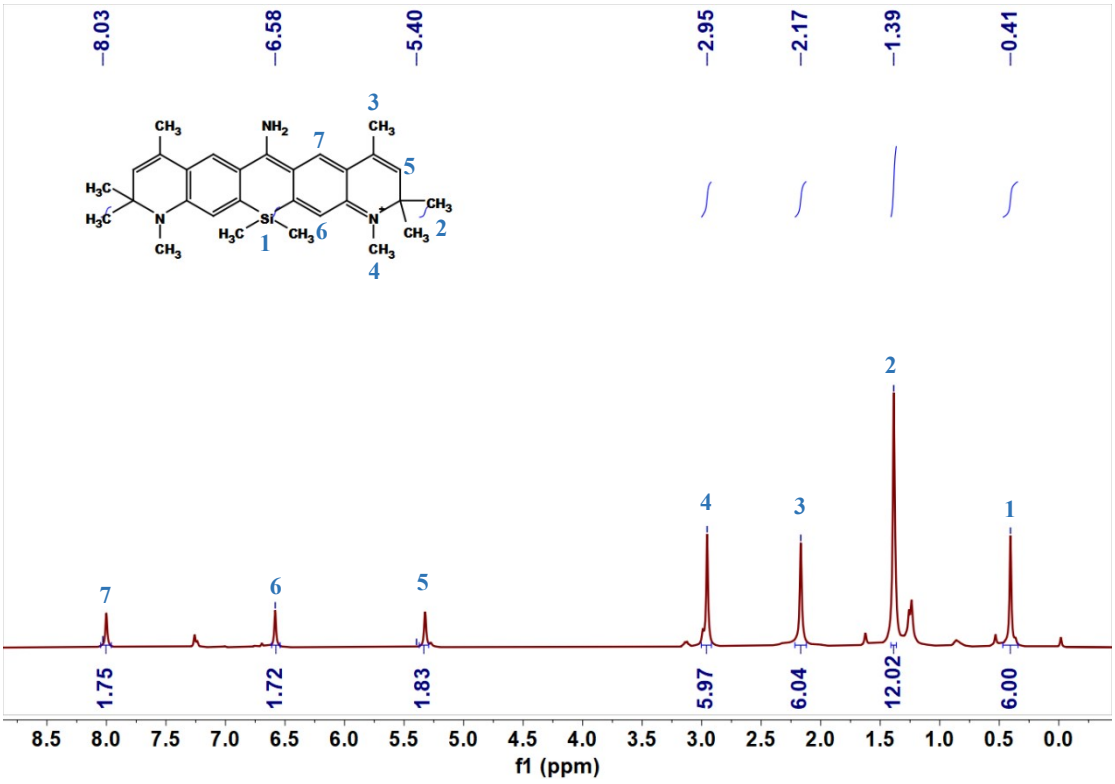

^{1}H NMR of **Si-NH$_2$** in $CDCl_3$

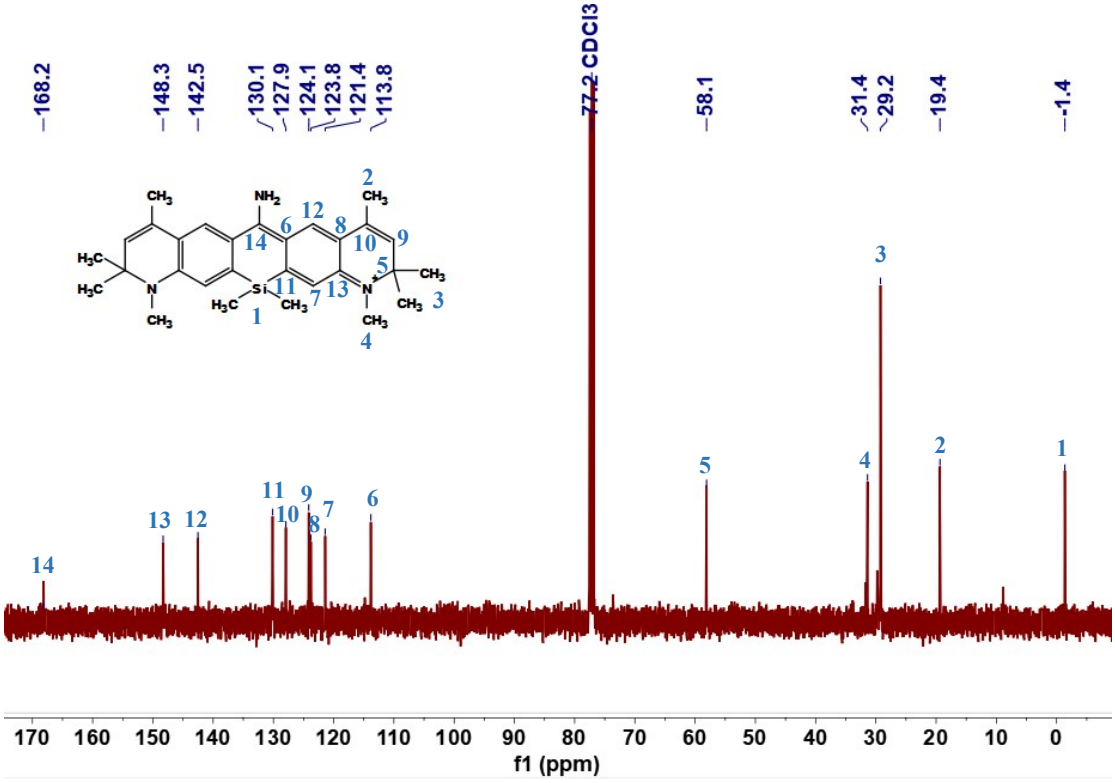

^{13}C NMR of **Si-NH$_2$** in $CDCl_3$

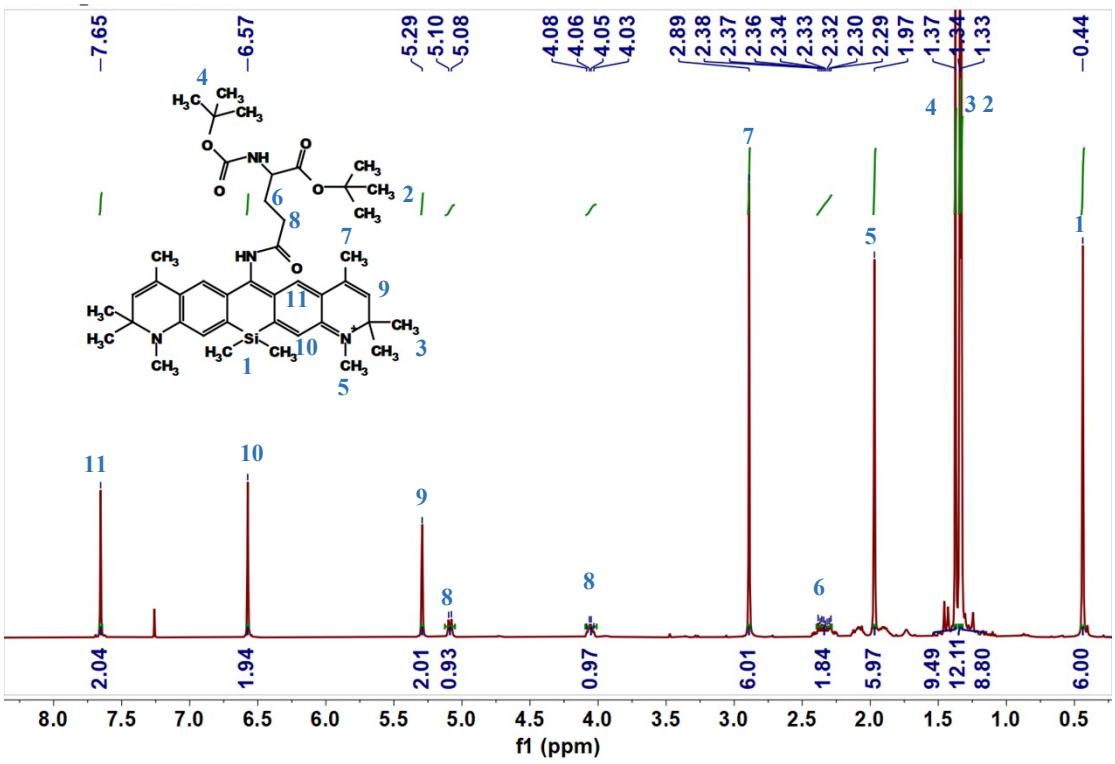

^{1}H NMR of **compound 8** in CDCl3

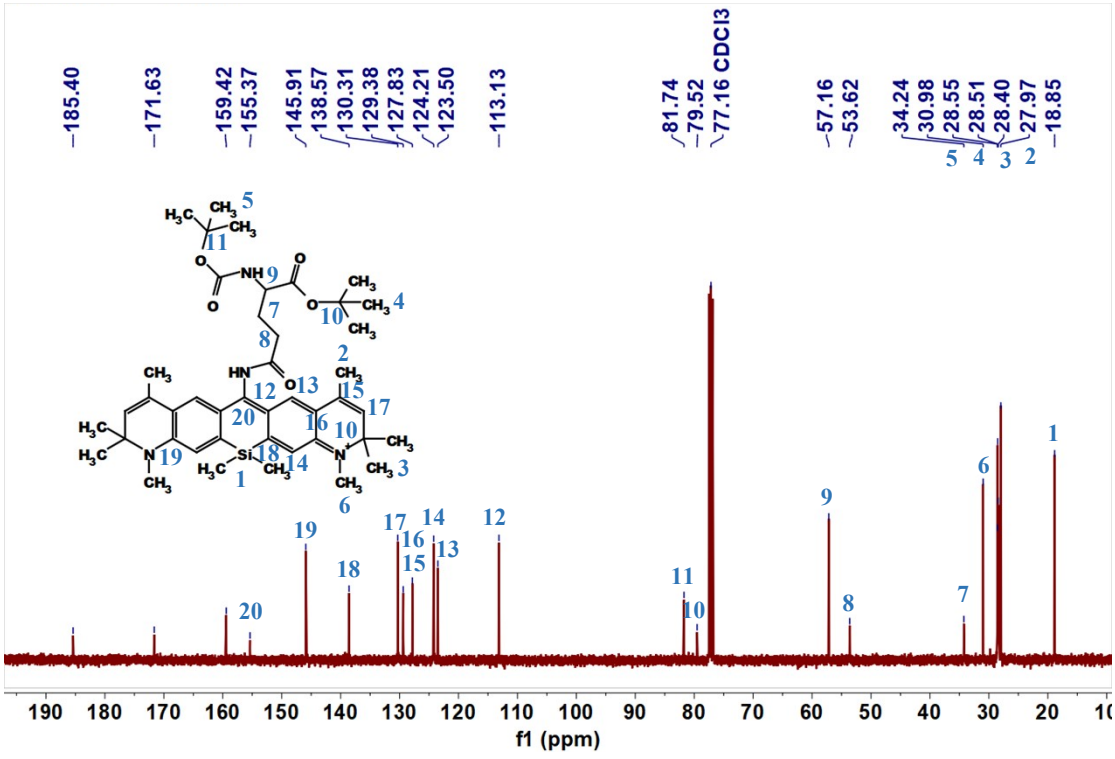

^{13}C NMR of **compound 8** in $CDCl_3$

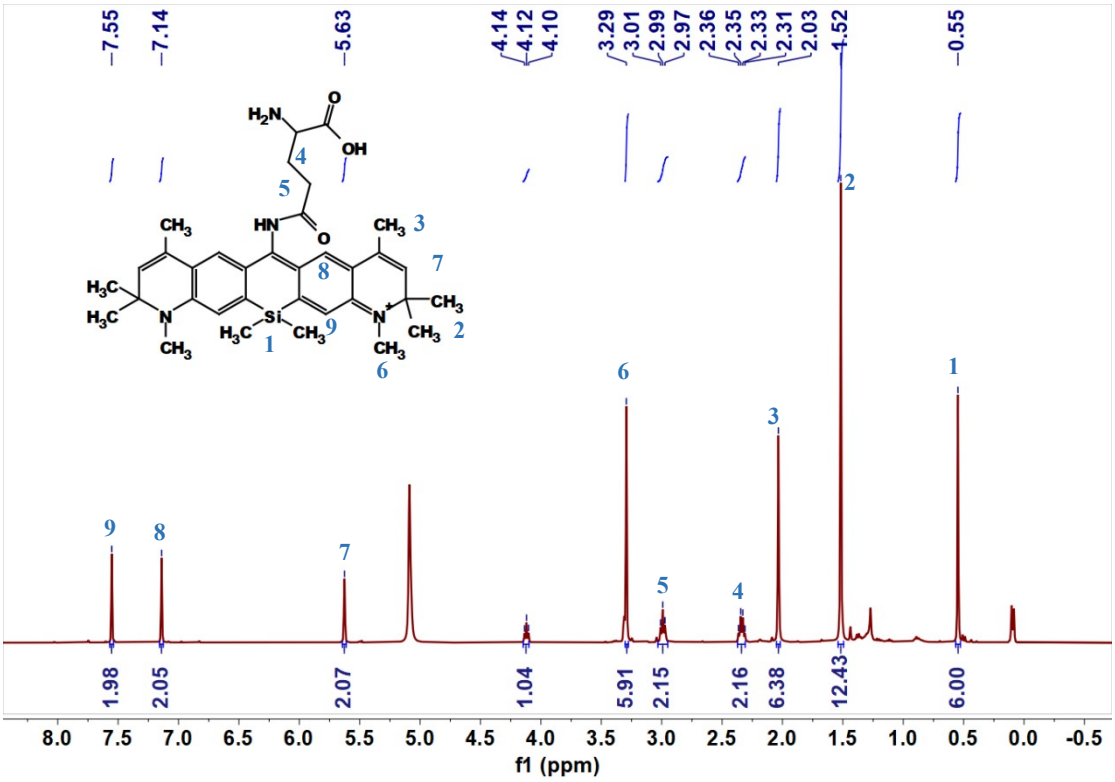

^{1}H NMR of **Si-NH$_2$-Glu** in CD$_3$OD

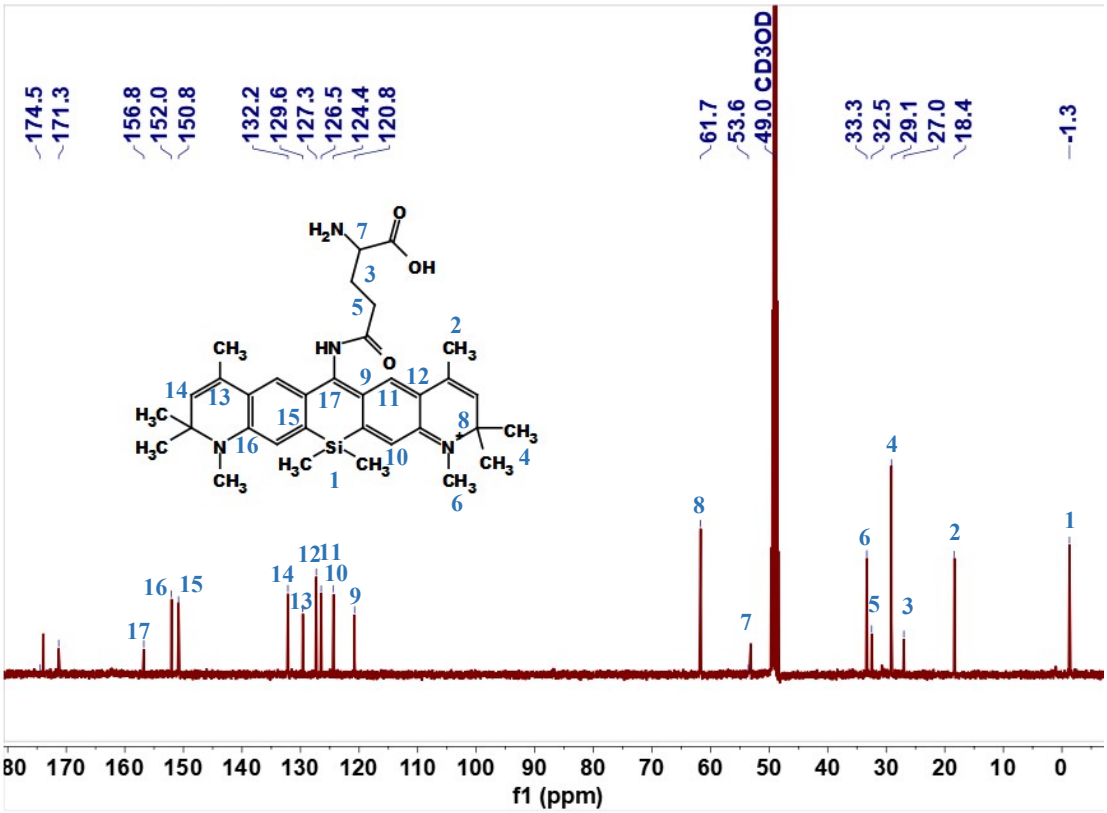

^{13}C NMR of **Si-NH$_2$-Glu** in CD$_3$OD

14. ESI-MS Data

Compound 6

ESI+

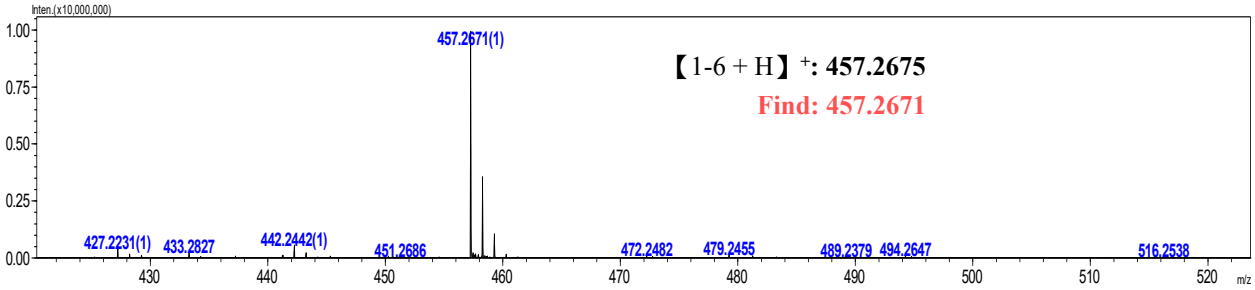

Si-NH_2

ESI+

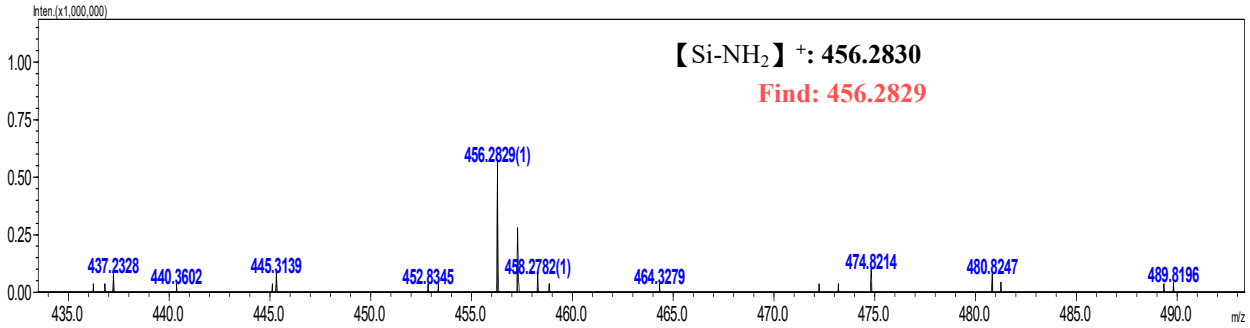

SI-NH_2-Glu

ESI+

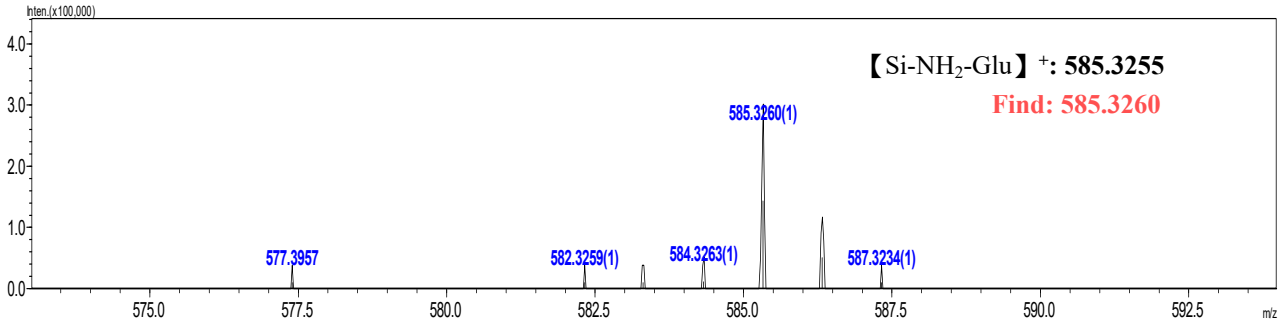

1 Y. Koide, Y. Urano, K. Hanaoka, W. Piao, M. Kusakabe, N. Saito, et al., Development of NIR Fluorescent Dyes Based on Si–rhodamine for in Vivo Imaging, J.Am.Chem.Soc., 2012, **134**, 5029- 50312

2 T. Lu and F. J. Comput. Chem, 2012, **33**, 580-592.

3 Z. Liu, T. Lu and Q. Chen, *Carbon*, 2020, **165**, 461-467.

4 X.-Y. Ran, P. Chen, Y.-Z. Liu, L. Shi, X. Chen, Y.-H. Liu, H. Zhang, L.-N. Zhang, K. Li and X. Q. Yu, Adv. Mater (2023). DOI: 10.1002/adma.202210179.